PERGAMON

International Journal of Heat and Mass Transfer 45 (2002) 3383–3396

International Journal of HEAT and MASS TRANSFER

www.elsevier.com/locate/ijhmt

Heat transfer and friction in solar air heater duct with V-shaped rib roughness on absorber plate

Abdul-Malik Ebrahim Momin [a,*], J.S. Saini [b], S.C. Solanki [b]

[a] *Industrial Technical Institute, Section B, Street No. 2, Auction-Bazaar, Crater-Aden, Republic of Yemen*
[b] *Department of Mechanical and Industrial Engineering, Indian Institute of Technology, Roorkee 247667, India*

Received 2 February 1999; received in revised form 31 December 2001

Abstract

In this work, results of an experimental investigation of the effect of geometrical parameters of V-shaped ribs on heat transfer and fluid flow characteristics of rectangular duct of solar air heater with absorber plate having V-shaped ribs on its underside have been reported. The range of parameters for this study has been decided on the basis of practical considerations of the system and operating conditions. The investigation has covered a Reynolds number (Re) range of 2500–18000, relative roughness height (e/D_h) of 0.02–0.034 and angle of attack of flow (α) of 30–90° for a fixed relative pitch of 10. Results have also been compared with those of smooth duct under similar flow conditions to determine the enhancement in heat transfer coefficient and friction factor. The correlations have been developed for heat transfer coefficient and friction factor for the roughened duct. © 2002 Published by Elsevier Science Ltd.

1. Introduction

Solar air heaters form the major component of solar energy utilization system which absorbs the incoming solar radiation, converting it into thermal energy at the absorbing surface, and transferring the energy to a fluid flowing through the collector. Solar air heaters because of their inherent simplicity are cheap and most widely used collection devices. These have found several applications including space heating and crop drying. The efficiency of flat plate solar air heater has been found to be low because of low convective heat transfer coefficient between absorber plate and the flowing air which increases the absorber plate temperature, leading to higher heat losses to the environment resulting in low thermal efficiency of such collectors. Several methods, including the use of fins, artificial roughness and packed beds in the ducts, have been proposed for the enhancement of thermal performance. Use of artificial roughness in the form of repeated ribs has been found to be a convenient method. Ribs of various shapes and orientations have been employed and the performance of such systems has been investigated. The use of artificial roughness in solar air heaters owes its origin to several investigations carried out in connection with the enhancement of heat transfer in nuclear reactors and turbine blades. Several investigations have been carried out to study the effect of artificial roughness on heat transfer and friction factor for two opposite roughened surfaces by Han [1,2], Han et al. [3–5], Lau et al. [6–8], Taslim et al. [9,10], Liou and Hwang [11], Han and Park [12] and the correlations were developed by different investigators.

Prasad and Mullick [13], Gupta [14], Saini and Saini [15] and Karwa [16] have carried out investigations on rib roughened absorber plates of solar air heaters that form a system with only one roughened wall and three smooth walls. Correlations for heat transfer coefficient and friction factor have been developed for such systems.

However, the increase in heat transfer is accompanied by an increase in the resistance of fluid flow. Many investigators [3,17,18] have studied this problem in an attempt to decide the roughness geometry which gives the best heat transfer performance for a given flow friction.

* Corresponding author.
E-mail address: abdulmalikmomin@yahoo.co.in (A.-M. Ebrahim Momin).

0017-9310/02/$ - see front matter © 2002 Published by Elsevier Science Ltd.
PII: S0017-9310(02)00046-7

Nomenclature

A_c	area of absorber plate (m^2)
C_p	specific heat of air (J kg^{-1} K^{-1})
D_h	hydraulic diameter of duct (m)
e	height of roughness element (m)
e/D_h	relative roughness height (dimensionless)
e^+	roughness Reynolds number (dimensionless)
f_r	average friction factor of roughened duct (dimensionless)
f_s	average friction factor of smooth duct (dimensionless)
H	height of the duct (m)
h	convective heat transfer coefficient (W m^{-2} K^{-1})
k	thermal conductivity of air (W m^{-1} K^{-1})
L	test length (m)
$\dot{m}$	mass flow rate of air (kg s^{-1})
Nu_r	average Nusselt number of roughened duct (dimensionless)
Nu_s	average Nusselt number of smooth duct (dimensionless)
p	rib pitch (m)
p/e	relative roughness pitch (dimensionless)
q	rate of heat transfer to air (W)
Re	Reynolds number (dimensionless)
St_r	average Stanton number of roughened duct (dimensionless)
St_s	average Stanton number of smooth duct (dimensionless)
$\overline{t_i}$	average inlet temperature of air (°C)
$\overline{t_o}$	average outlet temperature of air (°C)
$\overline{t_f}$	average temperature of fluid (°C)
$\overline{t_p}$	average temperature of absorbing plate (°C)
V	velocity of air in the duct (m s^{-1})
W	width of the duct (m)

Greek symbols

Δp	pressure drop in the test length (Pa)
ρ	density of air (kg m^{-3})
α	angle of attack of flow (°)

The application of artificial roughness in the form of fine wires on the heat transfer surface has been recommended to enhance the heat transfer coefficient by several investigators. Prasad and Mullick [13] used artificial roughness in the form of fine wires in a solar air heater duct to improve the thermal performance of collector and they have obtained the enhancement (ratio of the values for roughened duct to that for the smooth duct) in Nusselt number of the order of 1.385. Gupta [14] found that the heat transfer coefficient of roughened duct using wires as artificial roughness can be improved by a factor up to 1.8 and the friction factor has been found to increase by a factor up to 2.7 times of smooth duct. Saini and Saini [15] reported that a maximum enhancement in Nusselt number and friction factor for a duct roughened with expanded metal mesh is of the order of 4 and 5 respectively in the range of parameters investigated. Karwa [16] concluded that considerable enhancement of heat transfer can be obtained as a result of providing rectangular or chamfered rib roughness on the heat transferring surface of a rectangular section duct. The Stanton number has been found to increase by about 1.5–1.8 times for $W/H = 4.82$ and $e/D_h = 0.029$ and 1.7–2.1 times for $W/H = 7.75$ and $e/D_h = 0.044$ for $Re > 8000$ as compared to smooth duct. The corresponding values of increase in friction factor are 2–2.7 times and 2.9–3.1 times respectively. Prasad and Saini [19] reported that a maximum enhancement in Nusselt number and friction factor which are 2.38 and 4.25 times of smooth duct has been obtained by using artificial roughness. Cortes and Piacentini [20] have reported that incorporating wire-type periodic perturbations on the absorber plate of solar air heater enables efficiency improvements of 9–55% to be attained over the studied range of situations.

Although the heat transfer problems can be investigated by analytical means too, but due to the complex nature of governing equations and the difficulty in obtaining analytical/numerical solutions, the researchers have focused greater attention on the experimental investigation.

From the literature survey it was found that the Nusselt number on the ribbed side wall having transverse ribs is about two or three times higher than the four sided smooth channel values [1]. Han et al. [3] reported that ribs inclined at an angle of attack of 45° were found to have superior heat transfer performance when compared to transverse ribs. Han et al. [5], Lau et al. [6] and Taslim et al. [10] carried out investigation on rib roughened walls having V-shaped ribs and have reported that V-shaped ribs result in better enhancement compared to inclined ribs and transverse ribs. Lau et al. [6] reported that for the range of Reynolds numbers studied, the values of Stanton number in the 45° and 60° V-shaped ribs cases are 38–46% and 47–66% higher than those in the 90° full ribs case respectively and the pressure drop in 45° and 60° V-shaped ribs is 55–72% and 68–79% over the 90° full ribs respectively. They have also reported that the 60° V-shaped ribs have the higher ribbed wall heat transfer and thermal performance. The

45° and 60° V-shaped ribs also have higher ribbed wall heat transfer and pressure drop than corresponding angled full ribs (inclined ribs). Taslim et al. [10] have shown that the enhancement in heat transfer coefficient for air flow in a channel roughened with V-shaped ribs is on the average higher than that roughened with angled ribs as well as 90° ribs of the same geometry. The secondary flows generated and the favourable direction of vortices have been cited as the reasons for better performance of V-shaped ribs over that of others. The V-shaped ribs are tested for both pointing upstream and downstream of main flow. It has been shown that those pointing downstream are slightly better in performance. However, the difference has shown to be very small. Further, the effect of discreteness of the ribs on the performance has not been very pronounced.

The studies of Han et al. [5], Lau et al. [6] and Taslim et al. [10] have not covered the wide range of roughness and operating parameters as would be required for detailed analysis for detailed optimal design or selection of roughness parameter to be used in conventional solar air heaters. Further, the duct investigated has two opposite roughened walls whereas the solar air heaters are required to have a single heat transferring surface and hence a single artificially roughened wall. The present investigation was, therefore, taken up with the objective of extensive experimentation on V-shaped ribs as artificial roughness attached to the underside of one broad wall of the duct, to collect data on heat transfer and fluid flow characteristics. The data will be presented in the form of Nusselt number and friction factor plots as function of geometrical parameters of artificial roughness and thermo-hydraulic performance plots to bring out clearly the effect of these parameters and the enhancement in heat transfer achieved as a result of providing artificial roughness. The experimental data will be used to develop correlations for Nusselt number and friction factor for duct flow with one V-shaped rib roughened broad wall. These correlations can be employed by the designer for the selection of suitable roughness parameters for optimal enhancement of performance of solar air heater consistent with its system and operating parameters.

2. Experimental program and procedure

An experimental set-up has been designed and fabricated to study the effect of V-shaped ribs on heat transfer and fluid flow characteristics of flow in rectangular duct and to develop correlations for heat transfer coefficient and friction factor for the range of parameters decided on the basis of practical considerations of the system and operating conditions.

The experimental duct consists of an aluminium channel of 2.8 m long and 0.2 m wide which includes five sections, namely, smooth entrance section, roughened entrance section, test section, exit section and mixing chamber as Duffie and Beckman [21]. An aluminium sheet of 22 ASWG of 1.5×0.2 m^2 size was used as an absorber plate and the lower surface of the plate provided with artificial roughness in the form of V-shaped copper wires. An electric heater plate of identical dimensions as those of absorber plate was used to provide a uniform heat flux up to a maximum of 1500 W m^{-2} to the absorber plate. The power supply to the heater plate assembly was controlled through an AC variac.

A schematic diagram of the experimental set-up, a view of plate with roughness geometry, of 30° and 60° V-shaped ribs are shown in Figs. 1(a)–(d) respectively. The roughness elements used in the roughened plate are copper wires of different gauges. The V-shaped roughness elements were fixed below the absorbing plate and a fast drying epoxy applied for fixing the roughness elements and allowed to dry to ensure that the roughness elements were fixed properly with the surface of the plate.

The broad specifications and the range of roughness and flow parameters of the investigation are given in Table 1.

Seventeen roughened plates as detailed in Table 1 have been tested; each set consisting of 14 runs with different flow rates covering the Reynolds number range 2500–18000. Validity tests have also been conducted on a conventional smooth absorber plate under similar overall duct geometrical and flow conditions to serve as the basis of comparison of results with the values for heat transfer and friction factor from the correlations available for smooth duct in the literature.

The air is sucked through the rectangular duct by means of a blower driven by a 3-phase, 440 V, 3.0 kW and 2880 r.p.m., AC motor. It sucked the air through the duct and a gate valve has been used to control the amount of air in the duct. The air is thoroughly mixed in the mixing chamber before the exit temperatures were recorded and baffles were provided for achieving thorough mixing of the air. The duct was covered with thermocole (foamed polystyrene) from the three sides and upper side of the duct was covered with the thermocole and black insulating material, to ensure that all the heat flux which is supplied from the heater plate is transferred to the duct and also to minimize the losses to the surroundings. The other end of the duct is connected to a circular pipe via a rectangular to circular transition section.

The flow rate of air in the duct was measured by means of a flange type orifice meter calibrated by using a pitot tube, and the values of the coefficient of the discharge were obtained and used for calculating the flow rate of the air. Pressure drop across the orifice meter was measured by an inclined U-tube manometer with Spirit as manometric fluid.

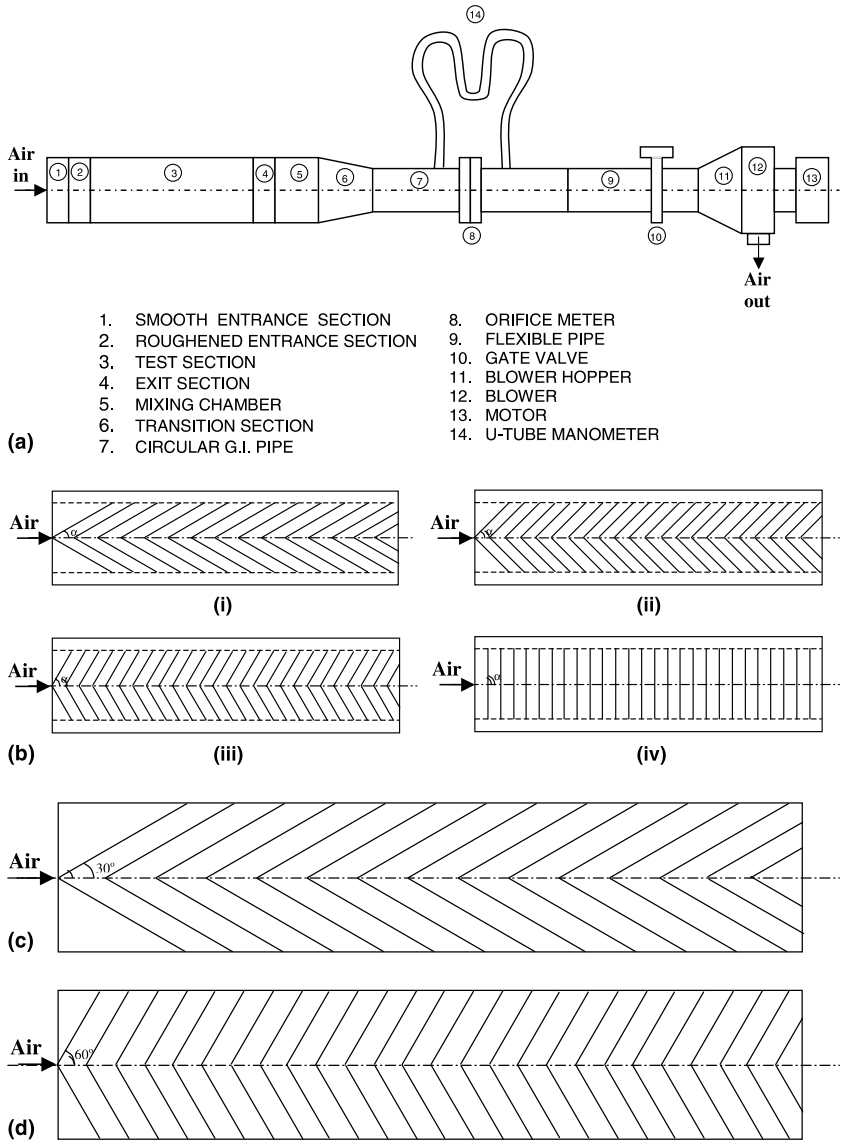

Fig. 1. (a) Schematic diagram of experimental set-up. (b) Roughness elements on absorber plate. (c) Schematic diagram of 30° V-shaped ribs. (d) Schematic diagram of 60° V-shaped ribs.

The pressure drop in the test section was measured by a micro-manometer having a least count of 0.005 mm. The micro-manometer consists of a movable reservoir and an inclined transparent tube connected to the movable reservoir through a flexible tubing. The reservoir is mounted on a sliding arrangement with a screw having a pitch of 1.0 mm and a graduated dial having 200 divisions, each division showing a movement of 0.005 mm of the reservoir. The two reservoirs were connected with the air taps of the duct through flexible tubes. The pressure difference across the two tappings was measured by moving the dial. Two pressure tappings fixed at inlet and outlet of test length (1.2 m) and connected to micro-manometer were used to measure the pressure drop across the test section.

Calibrated Copper Constantan (28 ASWG) thermocouples have been used for the measurements of average plate temperatures, average fluid temperatures in the duct, inlet and outlet air temperatures; the cold junction of the thermocouple is held at zero degree celsius by being placed into a thermo-flask containing an ice–water mixture. A digital microvoltmeter was used for the measurement of thermocouples output through the selector switch. Fig. 2(a) shows the position of the thermocouples on the absorbing plate and Fig. 2(b) shows the position of the thermocouples in the air duct.

Table 1
Broad specification and range of parameters of investigation

S. No.	e/D_h	α	Fixed parameters	Range of Reynolds numbers
1.	0.02	30°	$W/H = 10.15$	2500–18000
2.	0.02	45°	$p/e = 10$	(for each plate)
3.	0.02	60°	(for all the plates)	
4.	0.02	90°		
5.	0.022	30°		
6.	0.022	45°		
7.	0.022	60°		
8.	0.022	90°		
9.	0.028	30°		
10.	0.028	45°		
11.	0.028	60°		
12.	0.028	90°		
13.	0.034	30°		
14.	0.034	45°		
15.	0.034	60°		
16.	0.034	75°		
17.	0.034	90°		

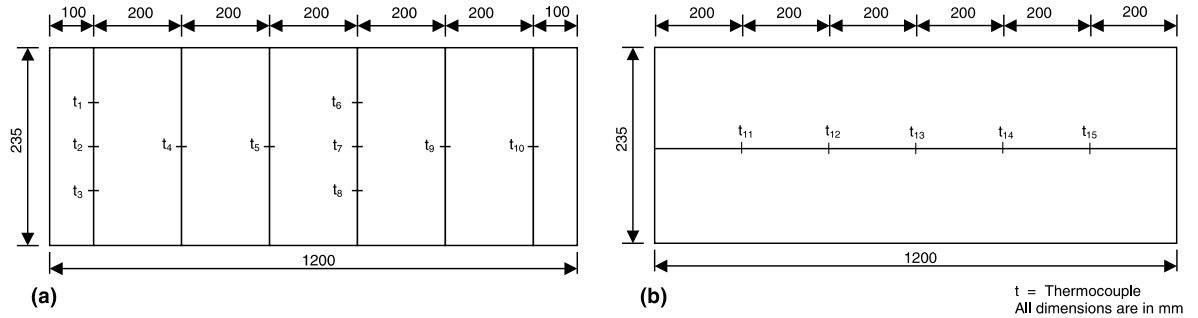

Fig. 2. (a) Position of the thermocouples on the absorbing plate (test length). (b) Position of the thermocouples in the air duct (test length).

Before starting the experiment all the thermocouples were checked carefully that they give the room temperature and all the pressure tappings were checked for the leakage problem.

After the ribs are installed and the test section is assembled, the energy for heating is supplied for one hour to the roughened entrance section and the test section. After 1 h the blower is switched on to let a predetermined rate of air flow through the duct. The steady state is attained in about 2 h when all the temperatures and pressures were recorded. The barometric pressure is assumed to be constant during the day.

3. Data reduction

Steady state values of the plate and air temperatures in the duct at various locations were obtained for a given heat flux and mass flow rate of air. Heat transfer rate to the air, Nusselt number and friction factor have been computed from the data. These values have been used to investigate the effect of various influencing parameters viz., the flow rate, the relative roughness height and the angle of attack of flow on the Nusselt number and friction factor.

The following equations have been used for the evaluation of relevant parameters:

$$q = m \times C_p \times (\overline{t_o} - \overline{t_i}), \tag{1}$$

$$h = q/[A_c \times (\overline{t_p} - \overline{t_f})], \tag{2}$$

$$Nu_r = (h \times D_h)/k, \tag{3}$$

$$f_r = D_h \times \Delta p/(2 \times L \times V^2 \times \rho). \tag{4}$$

The values of average Nusselt number (Nu_r) and friction factor (f_r) obtained under different roughness and flow conditions as described in Table 1 have been used to develop correlations and for the discussion of the effect of various parameters on heat transfer and flow friction.

An uncertainty analysis as proposed by Kline and McClintock [22] was used for prediction of the uncertainty which should be associated with an experimental result based on observations of the scatter in the raw data used in calculating the result. The following values give the uncertainty in the values of important parameters namely Reynolds number (Re), Nusselt number (Nu_r) and friction factor (f_r):

Parameter	Uncertainty (%)
Re	4.4
Nu_r	2.7
f_r	4.77

4. Results and discussion

Fig. 3 shows the variation of plate temperature and fluid temperature in the duct. The temperatures $\overline{t_p}$ and $\overline{t_f}$ are the average values of absorber plate temperature and fluid temperature respectively. The average value of plate temperature ($\overline{t_p}$) was determined from temperature measured at 10 locations on the plate as shown in Fig. 2(a). The average fluid temperature ($\overline{t_f}$) was determined from the values of the temperatures at five locations (central locations of duct cross-section along the flow direction). The average fluid temperature $\overline{t_f}$ was found from the readings of five thermocouples fixed in central locations of the duct cross-section along the flow direction, it was found that in the spanwise direction the variation of temperature was negligible. This variation is in agreement with work of Gupta [14] and Karwa [16].

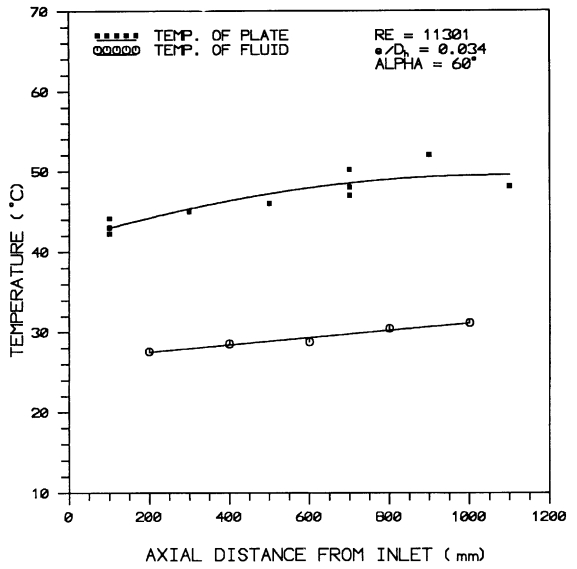

Fig. 3. Plate and air temperature distribution along the length of the test duct.

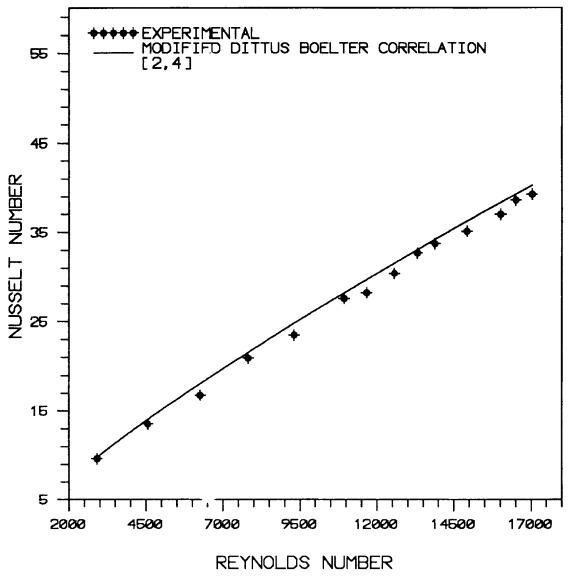

Fig. 4. Comparison of experimental values and predicted values of Nusselt number for smooth duct.

Figs. 4 and 5 show the comparison of the experimental values and those predicted by correlations for Nusselt number and friction factor of smooth duct proposed by Modified Dittus Boelter correlation for Nusselt Number and by Modified Blasius Correlation for friction factor. Altfeld et al. [23] suggested that modified Blasius correlation for friction factor can be used for smooth duct in solar air heater for Reynolds number

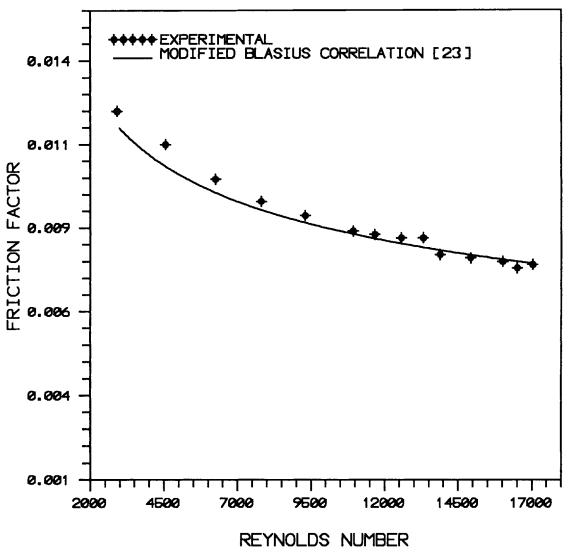

Fig. 5. Comparison of experimental values and predicted values of friction factor for smooth duct.

range applied for solar air heater. The modified Dittus Boelter correlation is applicable for $2500 < Re < 1.24 \times 10^5$ [24] and the minimum Reynolds number in our case is 2500.

For Nusselt number of smooth duct [2,4]

$$Nu_s = 0.023 \times Re^{0.8} \times Pr^{0.4} \times (2R_{av}/D_e)^{-0.2}, \quad (5)$$

where $2\ R_{av}/D_e = (1.156 + H/W - 1)/(H/W)$ for rectangular channel.

For friction factor

$$f_s = 0.085 \times (Re)^{-0.25}. \quad (6)$$

The absolute percentage deviation between the predicted and experimental results has been found to be 2.8% and 2.35% respectively for Nusselt number and friction factor. This comparison and resultant excellent agreement between the experimental and predicted values establish the accuracy of measurements on the experimental test rig.

The variations of Nusselt number and friction factor with Reynolds number, relative roughness height and angle of attack of flow are shown in Figs. 6–11. The results are discussed below.

4.1. Effect of Reynolds number

Figs. 6 and 9 show the effect of Reynolds number on Nusselt number and friction factor respectively. In general, Nusselt number increases whereas the friction factor decreases with an increase of Reynolds number as expected. However, the values of Nusselt number and friction factor are distinctly different as compared to those obtained for smooth absorber plates. This is due to a distinct change in the fluid flow characteristics as a result of roughness that causes flow separations, reattachments and the generation of secondary flows.

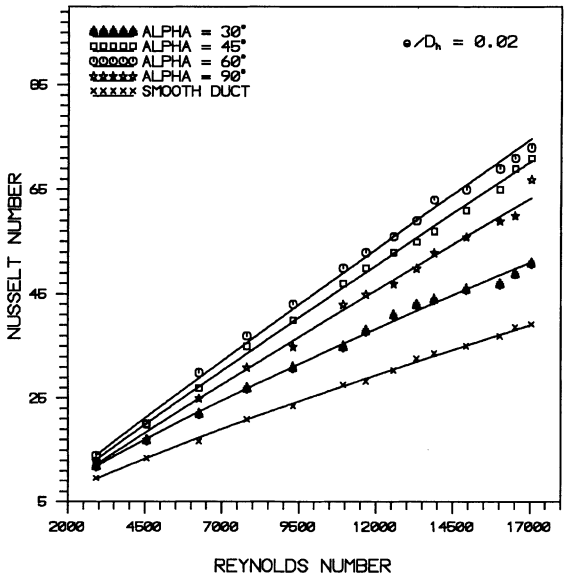

Fig. 6. Effect of Reynolds number on Nusselt number for relative roughness height of 0.02 and for given angle of attack of flow.

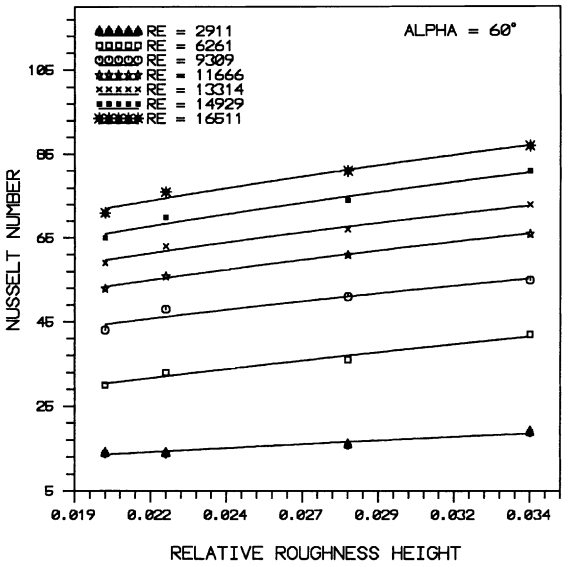

Fig. 7. Effect of relative roughness height on Nusselt number for given Reynolds number and for an angle of attack of flow of 60°.

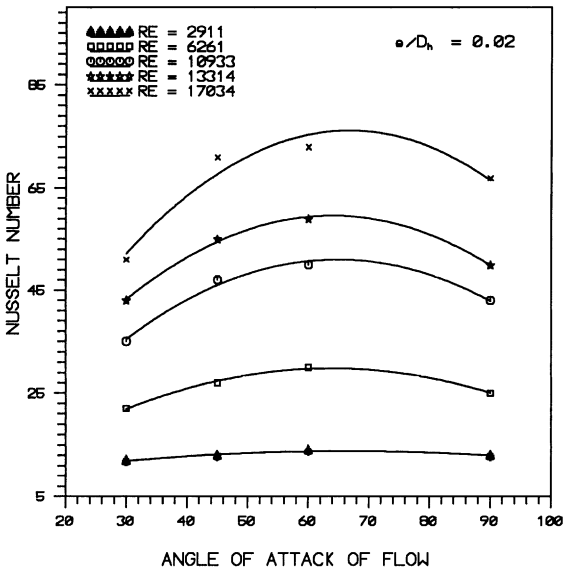

Fig. 8. Effect of angle of attack of flow on Nusselt number for relative roughness height of 0.02 and for given Reynolds number.

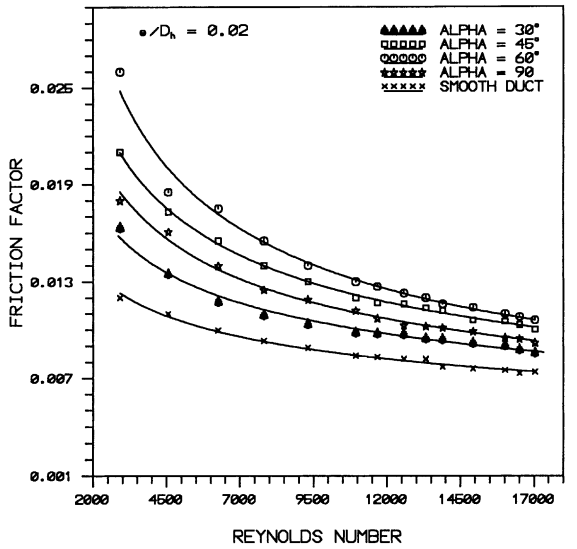

Fig. 9. Effect of Reynolds number on friction factor for relative roughness height of 0.02 and for given angle of attack of flow.

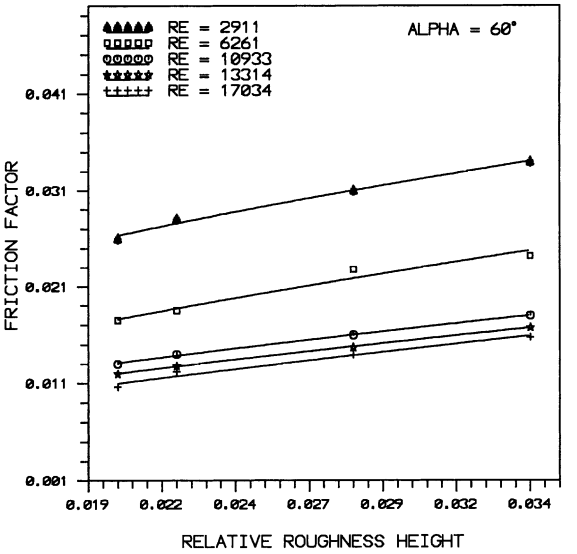

Fig. 10. Effect of relative roughness height on friction factor for given Reynolds number and for an angle of attack of flow of 60°.

In early studies carried out by Nikuradse and is given in the thesis of Gupta [14], he discussed the following flow regimes with respect to artificially roughened surfaces:

Range I: Hydraulically smooth flow regime $(0 \leqslant e^+ \leqslant 5)$;

Range II: Transitionally rough flow regime $(5 \leqslant e^+ \leqslant 70)$;

Range III: Completely rough flow regime $(e^+ > 70)$.

In hydraulically smooth flow regime i.e., for low Reynolds numbers the roughness has no effect on the friction factor for all the values of relative roughness height. The projections of the roughness elements lie entirely within the laminar sub-layer.

In transition rough flow regime, the influence of roughness becomes noticeable to an increasing degree. It is particularly characterized by the fact that the friction factor depends upon the Reynolds number as well as upon the relative roughness height. The thickness of laminar sub-layer is of the same order of magnitude as that of the height of roughness elements.

In completely rough flow regime, the friction factor becomes independent of the Reynolds number and the curve for friction factor vs. Reynolds number becomes parallel to the horizontal axis. All projections of the roughness elements extend beyond the laminar sub-layer as the thickness of boundary layer becomes small in comparison to the roughness height.

In our present investigation the flow lies in the transitionally rough flow regime. This flow is, therefore,

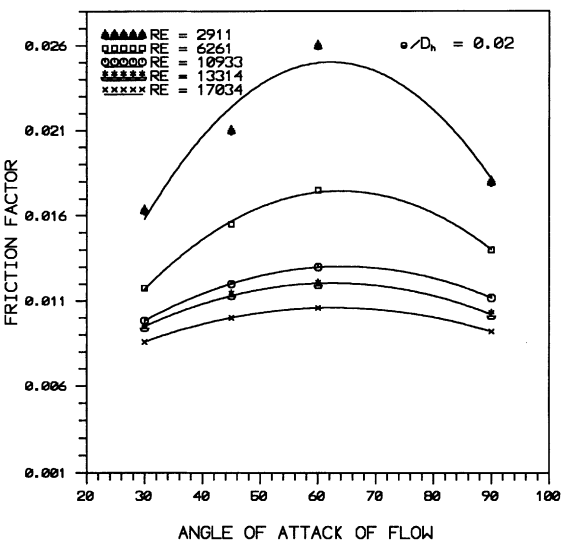

Fig. 11. Effect of angle of attack of flow on friction factor for relative thickness height of 0.02 and for given Reynolds number.

characterized by flow Reynolds numbers resulting in laminar boundary layers of thickness of the same order of magnitude as the roughness height. This is usually done to keep the friction losses in check although the highest Nusselt number values cannot be expected. However, as seen from Fig. 6, the enhancements are noticeable and justify the use of artificial roughness. The maximum enhancement of Nusselt number was found to

be 1.30, 1.81, 1.86 and 1.71 times that for smooth duct for angles of attack of 30°, 45°, 60° and 90° respectively for relative roughness height of 0.02. Whereas for relative roughness height of 0.034, the maximum enhancement in Nusselt number was found to be 1.66, 2.11, 2.30, 2.17 and 1.86 times for corresponding angles of attack of 30°, 45°, 60°, 75° and 90° respectively. Similarly, for relative roughness height of 0.02, the maximum enhancement in friction factor was found to be 1.36, 1.75, 2.17 and 1.50 times that of smooth duct for angles of attack of 30°, 45°, 60° and 90° respectively. Whereas for relative roughness height of 0.034, the maximum enhancement was found to be 2.02, 2.52, 2.83, 2.67 and 2.27 times for corresponding values of angles of attack of 30°, 45°, 60°, 75° and 90° respectively.

4.2. Effect of relative roughness height

The effect of relative roughness height on Nusselt number and friction factor is depicted in Figs. 7 and 10 respectively. It can be observed that the increase in relative roughness height results in an increase in heat transfer coefficient and the friction factor. It is seen that the rate of increase of Nusselt number is lower than that of the friction factor. This appears due to the fact that at relatively higher values of relative roughness height, the re-attachment of free shear layer might not occur and the rate of heat transfer enhancement will not be proportional to that of friction factor as stated by Gupta [14], Saini and Saini [15] and Prasad and Saini [19].

4.3. Effect of angle of attack of flow

The Nusselt number and friction factor as function of angle of attack of flow are shown in Figs. 8 and 11 respectively. The maximum enhancement of Nusselt number and friction factor as a result of providing artificial roughness has been found to be respectively 2.30 and 2.83 times that of smooth duct for an angle of attack of 60°. It is seen that there exists an angle of attack that corresponds to the maximum values of both Nusselt number and the friction factor. It appears that the flow separation in the secondary flow resulting from the presence of V-shaped ribs and the movement of resulting vortices combines to yield an optimum value of the angle of attack. The reasons for the occurrence of this maxima at 60° have not been yet investigated in detail. However the results are in broad agreement with previous investigations both on angled straight ribs [14] and V-shaped ribs [6].

5. Thermo-hydraulic performance

It has been found that the artificial roughness on the absorber plate of the roughened duct results in considerable enhancement of heat transfer. This enhancement is, however, accompanied by a substantial increase in friction factor. It is, therefore, desirable that to select the roughness geometry such that the heat transfer is maximized while keeping the friction losses at the minimum possible value. This requirement of the collector can be fulfilled by considering the heat transfer and friction characteristics simultaneously. A parameter that facilitates the simultaneous consideration of thermal and hydraulic performance is given by Webb and Eckert [25] as $(St_r/St_s)/(f_r/f_s)^{1/3}$. This parameter is plotted in Fig. 12 against Reynolds number for relative roughness height of 0.034 and for different angles of attack. It is seen that, in general, thermo-hydraulic performance improves with increasing angle of attack and absolute maxima occurs with an angle of attack of 60°. However for a given value of angle of attack, there is a maxima corresponding to a certain value of Reynolds number. It was found that as the relative roughness height is varied, the value of this parameter, in general increases with an increase of height in the range of values investigated as shown in Fig. 13.

Fig. 14 has been drawn to show the enhancement in the heat transfer achieved by using V-shaped geometry of roughness. The comparison of experimental values of Nusselt number as a function of Reynolds number has been drawn for V-shaped 60° ribs, inclined 60° ribs [14] and that for smooth absorber plate. It is seen that the V-shape enhances the values of Nusselt number by 1.14 and 2.30 over inclined ribs and smooth plate case at Reynolds number of 17034, while the corresponding

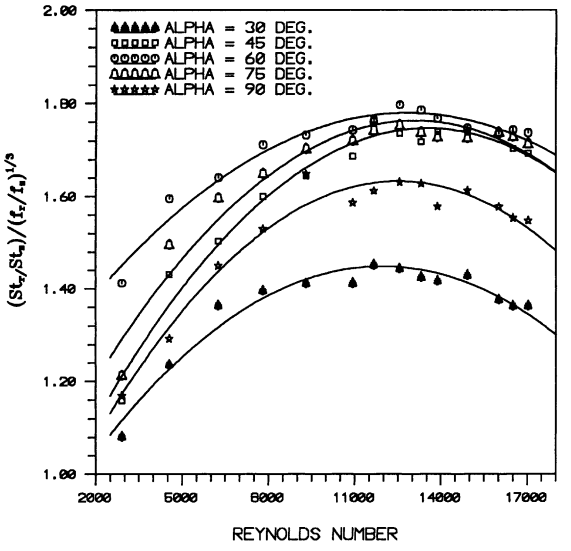

Fig. 12. Effect of Reynolds number on thermo-hydraulic performance parameter for relative roughness height of 0.034 and for given angle of attack of flow.

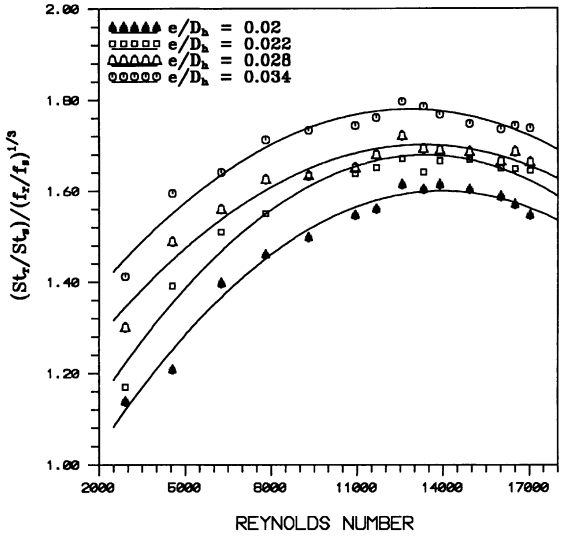

Fig. 13. Effect of Reynolds number on thermo-hydraulic performance parameter for angle of attack of 60° and for given relative roughness height.

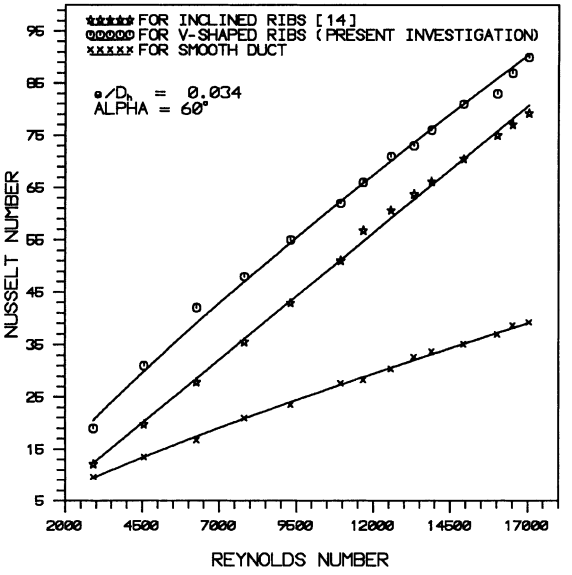

Fig. 14. Effect of Reynolds number on Nusselt number for inclined and V-shaped ribs for $\alpha = 60°$ and $e/D_h = 0.034$.

percentages of enhancement for a Reynolds number of 17034 are 12% and 56.4%.

6. Correlations for Nusselt number and friction factor

From Figs. 6–11, one can conclude that the Nusselt number and friction factor are strong functions of system and operating parameters of roughened duct, namely the Reynolds number (Re), relative roughness height (e/D_h) and angle of attack of flow (α). The functional relationships for Nusselt number and friction factor can therefore be written as

$$Nu_r = f(Re, e/D_h, \alpha), \tag{7}$$

$$f_r = f(Re, e/D_h, \alpha). \tag{8}$$

An attempt has been made to develop correlations as a function of system and operating parameters on the similar approach for making correlations by Saini and Saini [15] and Shou-Shing Hsieh et al. [26].

The data corresponding to all the 16 roughened plates totalling 224 data points were used for regression analysis to fit a second order polynomial.

Fig. 15 shows the Nusselt number as a function of Reynolds number. A regression analysis to fit a straight line through these data points as

$$Nu_r = A_1 \times (Re)^{0.888}. \tag{9}$$

Since the constant (A_1) will be a function of other parameters i.e. relative roughness height (e/D_h). So $Nu_r/Re^{0.888}$ ($= A_1$) is plotted in Fig. 16 as a function of relative roughness height (e/D_h), and by regression analysis it was obtained as

$$Nu_r/Re^{0.888} = A_2 \times (e/D_h)^{0.424}. \tag{10}$$

Further, the constant (A_2) will be a function of angle of attack (α), so the values of $Nu_r/[(Re)^{0.888} \times (e/D_h)^{0.424}]$ are plotted in Fig. 17 as a function of ($\alpha/60°$). On regression analysis to fit a second order polynomial, it was obtained as

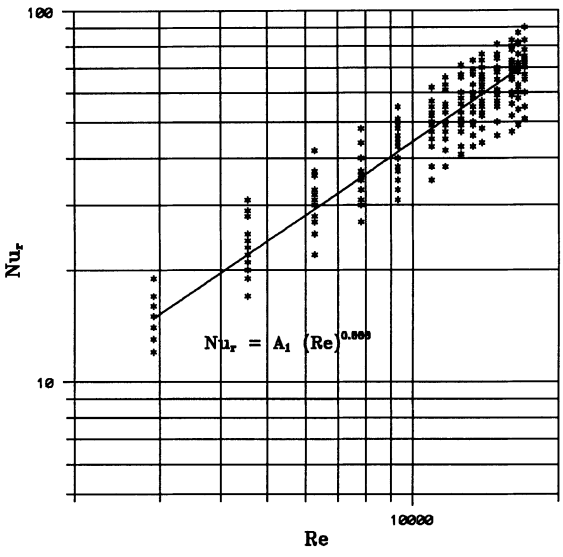

Fig. 15. Nusselt number vs. Reynolds number for 224 data points.

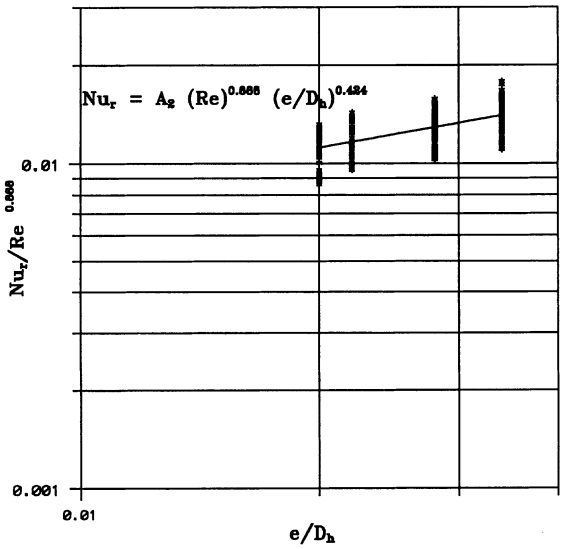

Fig. 16. Plot of $Nu_r/Re^{0.888}$ vs. e/D_h.

$$\log(Nu_r/(Re)^{0.888} \times (e/D_h)^{0.424}) = \log A_0 + A_1(\log \alpha/60^\circ) + A_2(\log \alpha/60^\circ)^2, \quad (11)$$

where A_0, A_1 and A_2 are constants obtained from regression analysis. Finally, converting Eq. (11) into appropriate form one can write as

$$Nu_r = 0.067 \times (Re)^{0.888} \times (e/D_h)^{0.424} \times (\alpha/60^\circ)^{-0.077} \times \exp[-0.782 \times (\ln \alpha/60^\circ)^2]. \quad (12)$$

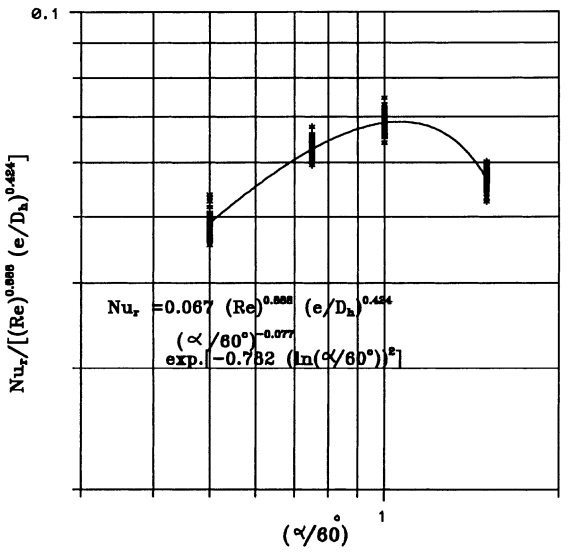

Fig. 17. Plot of $Nu_r/[Re^{0.888} \times (e/D_h)^{0.424}]$ vs. $(\alpha/60^\circ)$.

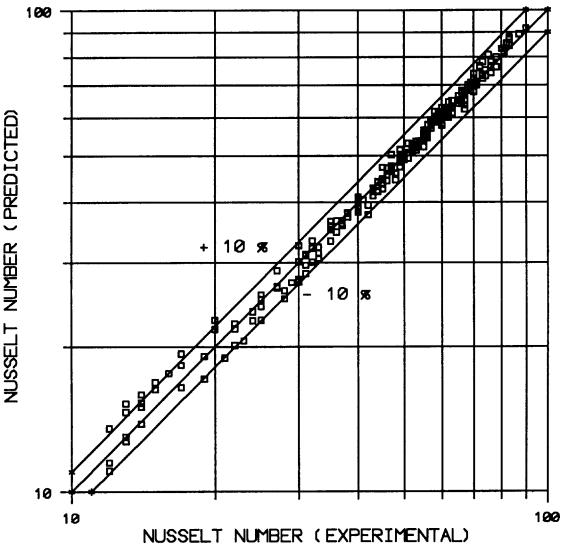

Fig. 18. Nusselt number (predicted) vs. Nusselt number (experimental).

The regression data relevant to this correlation are:

(a) Average absolute percentage deviation: 3.20;
(b) Regression coefficient: 0.97.

Fig. 18 shows the plot of experimental values and the values predicted using Eq. (12). It can be seen that 214 data points out of 224 data points lie within the deviation line ±10%.

A similar procedure has been employed and a correlation for friction factor has been developed. Figs. 19–21

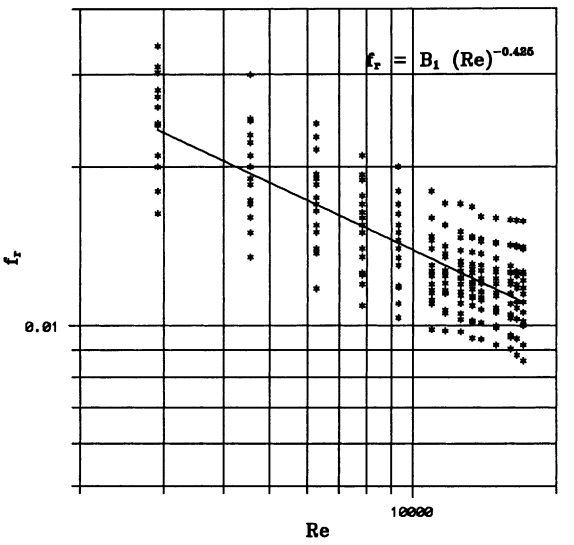

Fig. 19. Friction factor vs. Reynolds number for 224 data points.

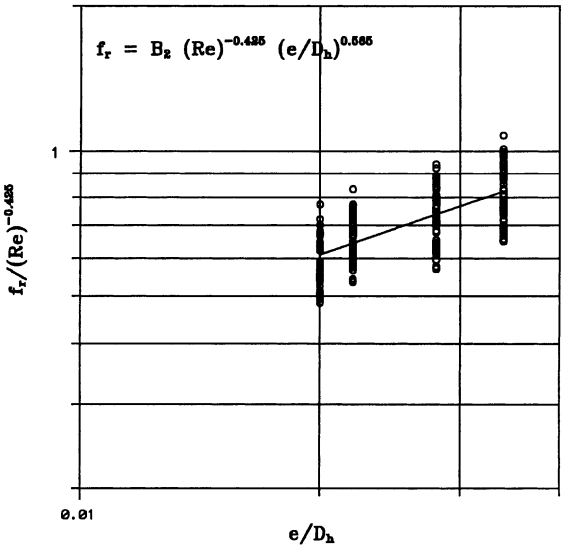

Fig. 20. Plot of $f_r/Re^{-0.425}$ vs. e/D_h.

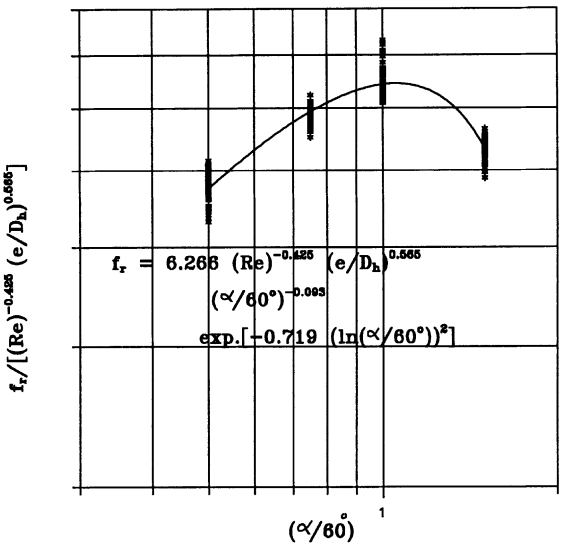

Fig. 21. Plot of $f_r/[Re^{-0.425} \times e/D_h^{0.565}]$ vs. $(\alpha/60°)$.

have been used to develop the correlation in the following form:

$$f_r = 6.266 \times (Re)^{-0.425} \times (e/D_h)^{0.565} \times (\alpha/60°)^{-0.093} \times \exp[-0.719 \times (\ln \alpha/60°)^2]. \quad (13)$$

The regression data relevant to this correlation are:

(a) Average absolute percentage deviation: 3.50;
(b) Regression coefficient: 0.93.

Fig. 22 shows the plot of experimental values and the values predicted using Eq. (13) for friction factor. It can be seen that 219 data points out of 224 data for friction factor lie within the deviation lines of ±10%.

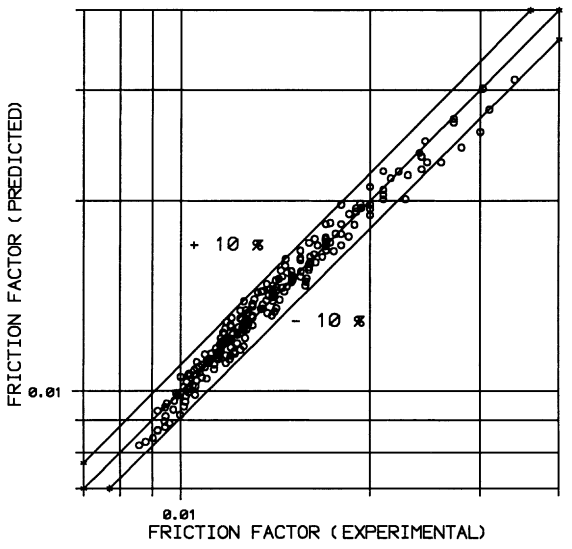

Fig. 22. Friction factor (predicted) vs. friction factor (experimental).

Hence, the correlations developed are reasonably satisfactory for the prediction of the Nusselt number and friction factor of roughened duct with fairly good accuracy in the range of parameters investigated.

It can be noted from correlations (12) and (13) that the effect of Reynolds number on Nusselt number and friction factor is much stronger as compared to that of the angle of attack as represented by a relatively higher exponent of Reynolds number in both these cases. This appears to be due to relative weakness of the influence of secondary flows that are created by the inclination of rib to the main flow. The secondary flow is cited to be the major cause of the change of Nusselt number and friction factor when angle of attack is changed.

Another notable difference lies in the effect of relative roughness height; the influence being more dominant in case of friction factor. As the relative roughness height increases, the chance of free shear layer re-attachment reduces thus causing a relatively weaker increase in heat transfer coefficient while strongly increasing the friction factor.

7. Conclusions

The following conclusions can be drawn from this work:

1. In general, Nusselt number increases whereas the friction factor decreases with an increase of Reynolds number. The values of Nusselt number and friction factor are substantially higher as compared to those

obtained for smooth absorber plates. This is due to distinct change in the fluid flow characteristics as a result of roughness that causes flow separations, re-attachments and the generation of secondary flows.

2. It was observed that the rate of increase of Nusselt number with an increase in Reynolds number is lower than the rate of increase of friction factor; this appears due to the fact that at relatively higher values of relative roughness height, the re-attachment of free shear layer might not occur and the rate of heat transfer enhancement will not be proportional to that of friction factor.
3. The maximum enhancement of Nusselt number and friction factor as a result of providing artificial roughness has been found to be respectively 2.30 and 2.83 times that of smooth duct for an angle of attack of 60°. It was observed that the same angle of attack corresponds to the maximum values of both Nusselt number and friction factor. It appears that the flow separation and the secondary flow resulting from the presence of V-shaped ribs and the movement of resulting vortices combine to yield an optimum value of angle of attack.
4. The thermo-hydraulic performance parameter improves with increasing the angle of attack of flow and relative roughness height and the maxima occurs with an angle of attack of 60°.
5. It was found that for relative roughness height of 0.034 and for angle of attack of 60°, the V-shaped ribs enhance the values of Nusselt number by 1.14 and 2.30 times over inclined ribs and smooth plate case at Reynolds number of 17034. It means that the V-shaped ribs have definite advantage over the inclined ribs for similar operating conditions.
6. The comparison of experimental values of Nusselt number and those predicted by the correlation shows that 214 out of 224 data points lie within the deviation range of $\pm 10\%$ whereas in the case of friction factor 219 out of 224 data points lie within $\pm 10\%$. It can therefore be concluded that the correlations are reasonably satisfactory for the prediction of Nusselt number and friction factor for the roughened duct.
7. It can be noted from the above correlations that the effect of Reynolds number on Nusselt number and friction factor is much stronger as compared to that of the angle of attack as represented by a relatively higher exponent of Reynolds number in both these cases.

References

[1] J.C. Han, Heat transfer and friction characteristics in rectangular channels with rib turbulators, ASME J. Heat Transfer 110 (1988) 321–328.

[2] J.C. Han, Heat transfer and friction in channels with two opposite rib-roughened walls, ASME J. Heat Transfer 106 (1984) 774–781.

[3] J.C. Han, L.R. Glicksman, W.M. Rohsenow, An investigation of heat transfer and friction for rib-roughened surfaces, Int. J. Heat Mass Transfer 21 (1978) 1143–1156.

[4] J.C. Han, J.S. Park, C.K. Lei, Heat transfer enhancement in channels with turbulence promoters, ASME J. Eng. Gas Turbines Power 107 (1985) 628–635.

[5] J.C. Han, Y.M. Zhang, C.P. Lee, Augmented heat transfer in square channels with parallel, crossed and V-shaped angled ribs, ASME J. Heat Transfer 113 (1991) 590–596.

[6] S.C. Lau, R.T. Kukreja, R.D. McMillin, Effects of V-shaped rib arrays on turbulent heat transfer and friction of fully developed flow in a square channel, Int. J. Heat Mass Transfer 34 (1991) 1605–1616.

[7] S.C. Lau, R.D. McMillin, J.C. Han, Turbulent heat transfer and friction in a square channel with discrete ribs turbulators, ASME J. Turbomachinery 113 (1991) 360–366.

[8] S.C. Lau, R.D. McMillin, J.C. Han, Heat transfer characteristics of turbulent flow in a square channel with angled discrete ribs, ASME J. Turbomachinery 113 (1991) 367–374.

[9] M.E. Taslim, L.A. Bondi, D.M. Kercher, An experimental investigation of heat transfer in an orthogonally rotating channel roughened with 45 deg. criss-cross ribs on two opposite walls, ASME J. Turbomachinery 113 (1991) 346–353.

[10] M.E. Taslim, T. Li, D.M. Kercher, Experimental heat transfer and friction in channels roughened with angled, V-shaped, and discrete ribs on two opposite walls, ASME J. Turbomachinery 118 (1996) 20–28.

[11] T.M. Liou, J.J. Hwang, Effect of ridge shapes on turbulent heat transfer and friction in a rectangular channel, Int. J. Heat Mass Transfer 36 (1993) 931–940.

[12] J.C. Han, J.S. Park, Developing heat transfer in rectangular channels with rib turbulators, Int. J. Heat Mass Transfer 31 (1988) 183–195.

[13] K. Prasad, S.C. Mullick, Heat transfer characteristics of a solar air heater used for drying purposes, Appl. Energy 13 (1983) 83–93.

[14] D. Gupta, Investigations on fluid flow and heat transfer in solar air heaters with roughened absorbers, Ph.D. Thesis. University of Roorkee, India, June 1993.

[15] R.P. Saini, J.S. Saini, Heat transfer and friction factor correlations for artificially roughened ducts with expanded metal mesh as roughness element, Int. J. Heat Mass Transfer 40 (1997) 973–986.

[16] R. Karwa, Investigation of thermo-hydraulic performance of solar air heaters having artificially roughened absorber plate, Ph.D. Thesis, University of Roorkee, India, March 1997.

[17] D.L. Gee, R.L. Webb, Forced convection heat transfer in helically rib-roughened tubes, Int. J. Heat Mass Transfer 23 (1980) 1127–1136.

[18] R. Sethumadhavan, M. Raja Rao, Turbulent flow heat transfer and fluid friction in helical wire-coil-inserted tubes, Int. J. Heat Mass Transfer 26 (1983) 1833–1844.

[19] B.N. Prasad, J.S. Saini, Effect of artificial roughness on heat transfer and friction factor in a solar air heater, Solar Energy 41 (1988) 555–560.
[20] A. Cortes, R. Piacentini, Improvement of the efficiency of a bare solar collector by means of turbulence promoters, Appl. Energy 36 (1990) 253–261.
[21] J.A. Duffie, W.A. Beckman, Solar Engineering of Thermal Processes, Wiley, New York, 1980.
[22] S.J. Kline, F.A. McClintock, Describing uncertainties in single sample experiments, J. Mech. Eng. 75 (1953) 3–8.
[23] K. Altfeld, W. Leiner, M. Fiebig, Second law optimization of flat-plate solar air heaters, Solar Energy 41 (1988) 127–132.
[24] Sadik Kakac, R.K. Shah, W. Aung, Hand Book of Single-Phase Convective Heat Transfer, Wiley, New York, 1987.
[25] R.L. Webb, E.R.G. Eckert, Application of rough surfaces to heat exchanger design, Int. J. Heat Mass Transfer 15 (1972) 1647–1658.
[26] Shou-Shing Hsieh, Huei-Jan Shih, Ying-Jong Hong, Laminar forced convection from surface-mounted ribs, Int. J. Heat Mass Transfer 33 (1990) 1987–1999.